Hindawi
International Journal of Polymer Science
Volume 2023, Article ID 1240792, 16 pages
https://doi.org/10.1155/2023/1240792

Research Article

The Influence of Glass Fiber/Glass Fiber Powder with β-Nucleating Agent on the Properties of Polypropylene

Peng Yan,[1] **Shaoran Kang**,[1,2] **and Lebo Ma**[1]

[1]*Ningxia Shenyao Technology Co., Ltd, Yinchuan, Ningxia Hui Autonomous Region 750004, China*
[2]*College of Bioresources Chemical and Materials Engineering, Shaanxi University of Science and Technology, Xi'an 710021, China*

Correspondence should be addressed to Peng Yan; tureyp@qq.com

Received 3 November 2022; Revised 28 February 2023; Accepted 16 March 2023; Published 27 March 2023

Academic Editor: Maria Laura Di Lorenzo

Glass fiber-reinforced polypropylene (PP/GF) has been widely used due to its high stiffness, but for some applications that need low-module characteristics, PP/GF will have limitations due to its lower toughness, so it is necessary to develop glass fiber-modified polypropylene with good stiffness–toughness balance performance. In this study, two average length glass fibers (4.5 mm and 12 mm) and glass fiber powder, combined with β-nucleating agent, were used to investigate the effects on the crystallization and mechanical properties of polypropylene. The results show that compared with glass fiber, glass fiber powder cooperates with β-nucleating agent reinforced polypropylene composite showed good stiffness–toughness balance performance, and β-crystals were found in the composite measured by Differential Scanning Calorimetry (DSC), the presence of β-crystals can improve the toughness of the composite.

1. Introduction

At present, glass fiber-reinforced polypropylene (PP/GF) has been widely used all over the world due to its good stiffness and cost-effective, but its toughness needs to be further improved to meet more application scenarios. The different characters of GF will influence on properties of PP/GF, and GF modification is an important research direction, various methods of modification or parameter adjustments for GF, such as lengths adjustments, surface treatments, and coupling agents, have an impact on the properties of modified PP [1–11]. Among them, in practical application, GF length is the most parameter that can be easily regulated. In industrial applications, GF can be classified as short GF (≤6 mm), long GF (6–25 mm), continuous glass fiber (CGF), and glass fiber powder (GFP) according to the average length and particle morphology, and the relative modification effects are obviously different.

Thomason and Vlug [1] systematically studied the effect of GF length on the properties of PP, they found that as the GF content increases, the parameters of stiffness such as tensile modulus and tensile strength increase linearly, and when the wt% concentration is greater than 40%, the rate of increase will be lower, the author explained that such phenomenon is since more GFs agglomerate, which lowers the stiffness increasing effect. They also found that when the GF wt% concentration is greater than 40%, the rate of stiffness parameters increasing began to decline, which the authors believe is because more fibers agglomerate and reduce the strengthening effect. For the GF length, they discovered that when the average fiber length is greater than 0.5 mm, agglomeration is obvious that affects reinforced effect under high GF concentration, but shorter fibers can achieve higher content filling, because agglomeration can be avoided to a certain extent as the GF length decreases. In terms of toughness, Thomason and Vlug [5] found that with the increase of GF concentration and length, the Charpy notched impact strength increased, but when the length exceeded 6 mm, the increasing trend is different, which indicates that the length of GF has different reinforced effects on the performance of PP composites, and the influence mechanism will change.

The material processing process will have influence on the length of the GF. During the processing using twin-

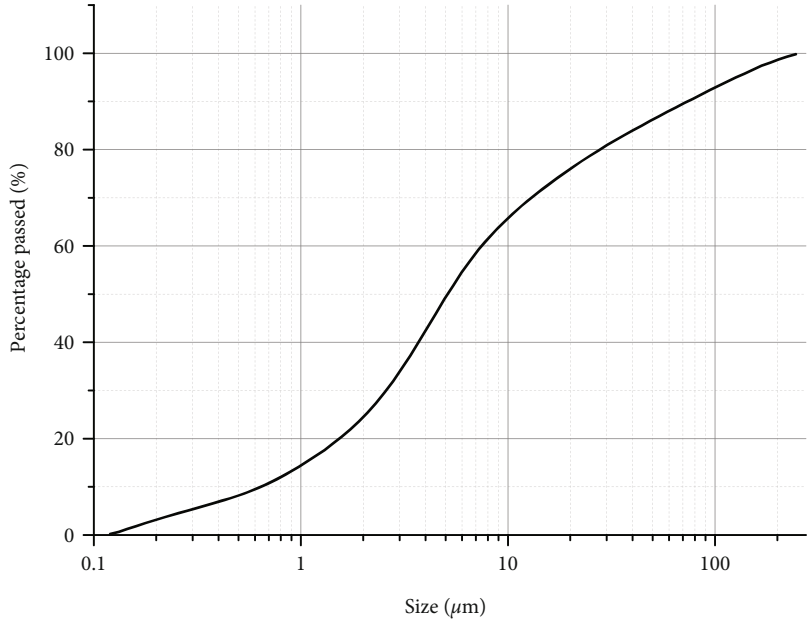

Figure 1: Particle size distribution glass fiber powder.

Table 1: Compositions of the samples (mass ratio).

Sample	WBG-II	GF-L	GF-S	GF-P
PP/WBG	0.2			
PP/GF-L		20		
PP/GF-S			20	
PP/GF-P				20
PP/WBG/GF-L	0.2	20		
PP/WBG/GF-S	0.2		20	
PP/WBG/GF-P	0.2			20

screw, the high shear force will cut off part of the GF to form a short with an average length of less than 1 mm, which will have an impact on the strengthening and toughening properties of PP composite [12]. However, to maintain the relative length of GF during processing, it is necessary to use a special processing process with low-shear force to GF, and its complex processes and equipment result in costs increasing, which is unfavorable for the promotion of industrial production. Therefore, it is necessary to carry out research to investigate the influence of GF length and morphology on the PP composites properties in ordinary processing equipment of twin-screw extruder.

Compared with GF, the average particle size of GFP is in the micron range, and the relevant properties have changed significantly because the basic morphology has changed from two dimensions to one dimension. For the research of GFP-modified PP, numerous studies have focused on nano-SiO_2 for its unique nano properties, and it can improve mechanical properties and temperature resistance to a certain extent under relative low concentration; however, the enhancement effect is limited compared to GF [13–15], nano-SiO_2 is expensive, therefore, for cost performance, it is necessary to do research focus on GFP. The average particle size of GFP is at the millimeter level with a broad particle size distribution, its modification performance and mechanism for PP will be different from the nano-SiO_2. However, relatively few studies have been reported in this area.

PP/GF has excellent mechanical properties like tensile strength and flexural modulus, but there are certain limitations in some applications that low modulus and surface flatness are required. Therefore, it is necessary to reduce the modulus while maintaining toughness under the premise of maintaining high mechanical properties. Therefore, various elastomers can be added to PP/GF [16–18], or nucleation modification can be carried out using β-nucleating agent (β-NA) [19, 20].

Based on practical application, in this study, we focus on the GF-modified PP, to study the influence of different types of GFs on the properties of PP composite. Three GF materials with different lengths and morphology were used: 4.5 mm short GF, 12 mm long GF, and GFP, and their synergy effects with β-NA were also investigated.

2. Experimental

2.1. Materials. The isotactic PP (trade mark 1100N) was produced by China Energy Group Ningxia Coal Industry Co., Ltd, with a density of 0.9 g/cm^3 and Meltmass-flowrate (MFR) of 3.57 g/10 min (230°C/2.16 kg). Three types of GFs were provided by China Jushi Group, two of them have an average diameter of 4.5 mm (term GF-S) and 12 mm (term GF-L), one is glass fiber powder (term GF-P) that its particle size distribution measured by laser particle analyzer (Microtraclnc-3500, America) represented in Figure 1, from which it can be seen that GF-P with a wide particle size distribution, the finest particles reach about 120 nm, and ≤1 μm

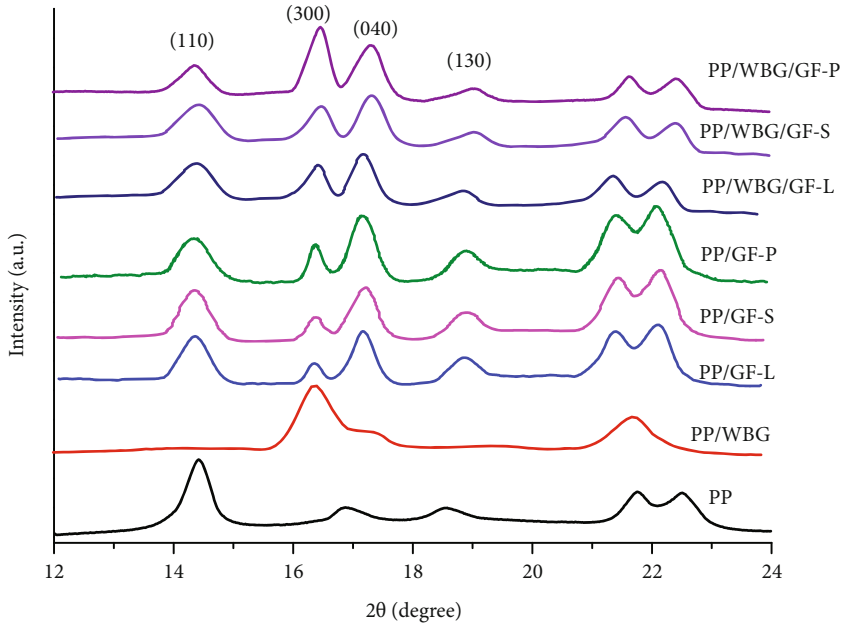

Figure 2: XRD diffraction patterns of samples.

particle size distribution section accounts for a certain proportion. Silane coupling agent KH-570 was purchased from Sinopharm Chemical Reagent Co., Ltd. β-NA with brand name WBG-II (term as WBG or β-NA) was purchased from Guangdong Weilinna New Material Technology Co., Ltd, China, it is a commercially sold rare earth-based nucleating agent material. Antioxidant (trade mark B215) was produced from BASF.

2.2. Sample Preparation. The concentrations of β-NA, antioxidant, and KH-570 are fixed at 0.2 wt%, 0.1 wt%, and 3 wt%, respectively, and in this study, the optimal concentration of 0.2 wt% for β-NA and 3% for KH-570 were proved by results of previous studies [21, 22]. Firstly, β-NA and antioxidant blended with iPP in a SHR 50A high-speed mixer (Zhangjiagang Jurun Machinery Co., Ltd) mixing for 5 minutes, the materials obtained above were extruded and pelletized in a SK36 twin-screw extruder (Nanjing KY Chemical Machinery Co., Ltd.), the barrel temperatures were set at 160–220°C from hopper to die with 60 rpm screw speed. Secondly, the above obtained pellets were melt blended with the GF and KH570 using the same process except that the screw speed was set at 10 rpm to minimize fiber damage. The composition of the different test materials is listed in Table 1.

2.3. Characterizations and Measurements. Standard tensile measurements and flexural tests were conducted by using a universal materials tester (WDT-W-20A, Chengde Precision Testing Machine Co., Ltd., China). The dumbbell-shaped specimens for the tensile tests were performed according to ASTM D-638 (type I) at a crosshead speed of 50 mm/min with a gauge length of 50 mm. Static flexural tests were measured using a three-point bending set up according to ASTM D-790 under cross head speed of 2 mm/min, and its dimensions were $127 \times 12.7 \times 3.0\,\text{mm}^3$, the notched Izod impact strength of the specimens was tested according to ASTM D-256 with Impact Testing Machine (XJC-5D, Chengde Precision Testing Machine Co., Ltd., China). The specimens' dimensions were $63.5 \times 12.7 \times 33.0\,\text{mm}^3$ with a "v" notch. All mechanical tests were carried out at room temperature. For each specimen, five measurements were taken and average results were calculated.

The melting and crystallization behavior of the samples were investigated on a thermal analysis apparatus (Differential Scanning Calorimetry (DSC) 214, NETZSCH) under nitrogen atmosphere. The mass of all samples subjected to DSC operation was approximately 4.0 mg and was sealed in a small dish made of aluminum. First, use indium to calibrate the heat flow and temperature. When studying the DSC behavior of samples, the temperature rise and fall rates of the samples were all set to $10^\circ\text{C min}^{-1}$. Firstly, the samples were heated to 200°C at an initial temperature of 50°C and held there for 5 minutes to obtain an amorphous melt and eliminate its thermal memory. Secondly, reduce the samples from a temperature of 200°C to 50°C. Finally, increase the temperature to 200°C again. The melting enthalpy of each phase obtained by DSC is represented by ΔH_i and the methods proposed by Li and Cheung [23]. The relative crystallinity is defined in Equation (1)

$$X_t = \frac{X_t(t)}{X_t(\infty)} = \frac{\int_0^t (\mathrm{d}H/\mathrm{d}t)\,\mathrm{d}t}{\int_0^\infty (\mathrm{d}H/\mathrm{d}t)\,\mathrm{d}t}, \quad (1)$$

where $X_t(t)$ and $X_t(\infty)$ represent the absolute crystallinity at time t and termination.

Wide angle X-ray diffraction (XRD) patterns of the nucleated iPP samples were recorded in an X-ray diffractometer (ARL EQUINOX 100 X, Thermo Fisher), it was

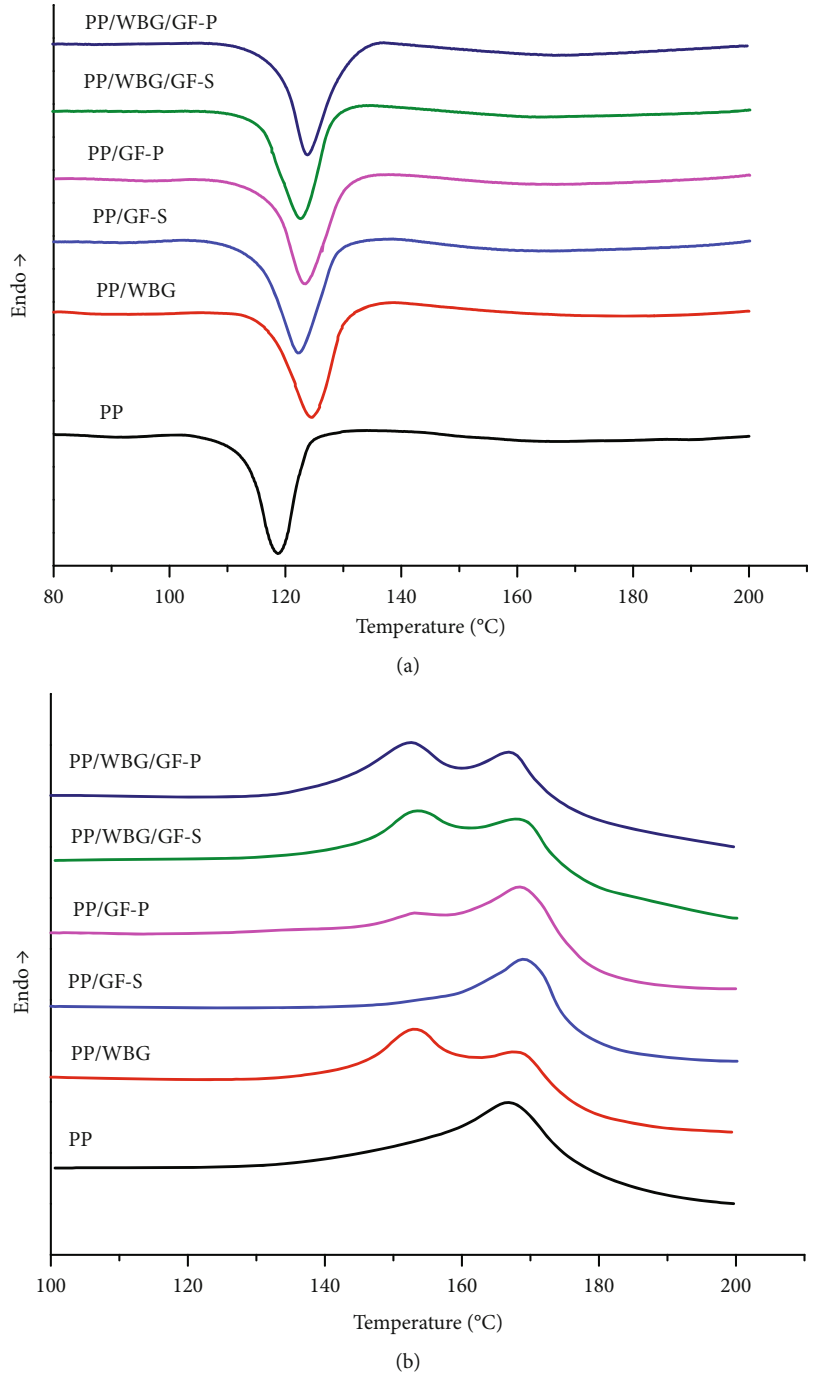

Figure 3: DSC (a) cooling and (b) heating of samples.

Table 2: Crystallization and melting parameters of samples.

Sample		PP	PP/WBG	PP/GF-S	PP/GF-P	PP/WBG/GF-S	PP/WBG/GF-P
Crystallization	T_{cp} (°C)	119.2	124.9	122.0	123.4	122.2	124.0
	ΔH_c (J/g)	81.2	85.6	76.3	77.2	72.1	74.8
Melting	$T_{\alpha m}$ (°C)	168.0	168.5	169.4	168.4	168.4	166.8
	$\Delta H_{\alpha m}$ (J/g)	157.3	149.5	157.4	156.2	155.2	155.3
	$T_{\beta m}$ (°C)	—	152.8	—	153.0	153.4	152.6
	$\Delta H_{\beta m}$ (J/g)	—	62.8	—	15.5	41.5	53.7

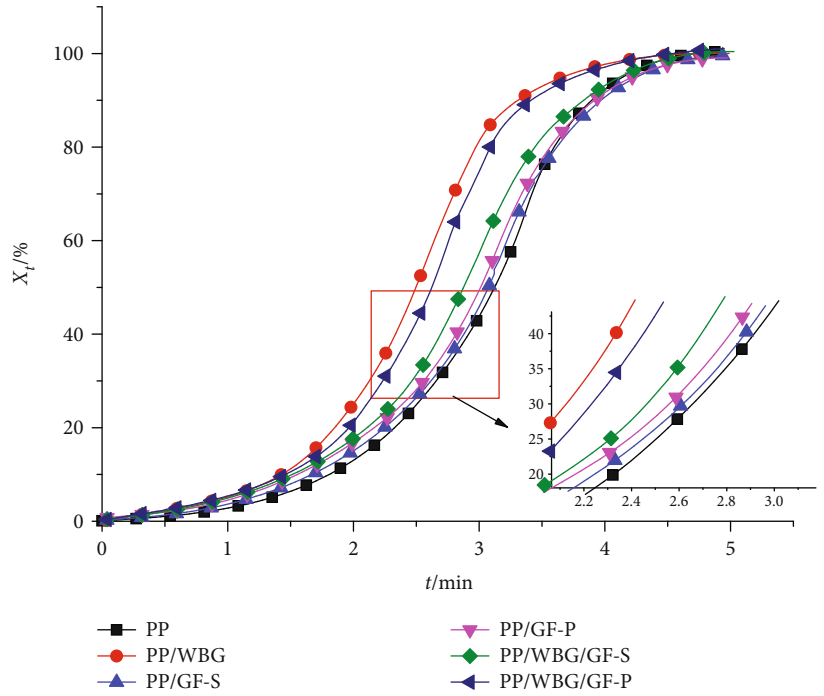

Figure 4: The variation in the relative degree of crystallinity (X_t) values as a function of crystallization time (t) for samples at a cooling rate of 5°C/min.

Table 3: $t_{2/1}$ of samples.

Sample	PP	PP/WBG	PP/GF-S	PP/GF-P	PP/WBG/GF-S	PP/WBG/GF-P
$t_{1/2}$ (min)	3.01	2.48	2.97	2.93	2.75	2.56

operated at a voltage of 40 kV and a filament current of 30 mA. Radial scans of intensity versus diffraction angle (2θ) were recorded in the range of 10–24°. The scanning rate was 4°/min.

3. Result and Discussion

3.1. Crystallization. The XRD spectrum of all samples is shown in Figure 2. Compared with pure PP, PP/WBG has obvious response peak at 16.1°, which corresponds to the β-crystals of the (300) lattice plane, indicating that β-NA can effectively increase the β-crystals content in the composite. The β-crystals response intensity is different, among which the PP modified by the GF-L and GF-S have basically similar XRD patterns, while the intensity of GF-P is slightly greater than the other two, which indicates that GF-P is conducive to promoting the formation of a certain content of β crystallization. Wang et al. [22] used KH570 as a coupling agent and nano-SiO_2 to modified PP, and found that when the mass fraction of nano-SiO_2 exceeded 1%, β-crystals corresponding peaks appeared in XRD, and as the amount of nano-SiO_2 increased, the β-crystals response intensity was enhanced. Wang et al. [22] synthesized nano-SiO_2/PP composites by pre-stretching technology, and also found that under certain conditions, the presence of nano-SiO_2 will promote the formation of β crystallization in PP. In this study, the average particle size of the GFP used was about 10 microns, which indicates that micron-level SiO_2 also has a certain role in promoting β crystallization. In addition, it can be seen from the particle size distribution in Figure 1 that due to the wide particle size distribution of GF-P, some very fine particles have reached the nanometer level, and the finest particle diameter is only about 120 nm, and these small amounts of nano-scale SiO_2 may also be the main reason for the formation of β crystallization. When using β-NA and GF in synergy, it can be clearly seen that the intensity of the corresponding peak of β-crystals is further increased compared with that of β-NA not added, indicating that more β-crystals are formed by adding β-NA to GF. When β-NA is added to PP/GF, the β-crystals response intensity of GF-S and GF-L is basically close, but with GF-P is more intense, which indicates that β-NA and GF-P have a good synergistic effect of promoting the transformation of β crystallization.

The XRD spectra of GF-L and GF-S are basically the same, and the results of other measurements such as DSC and mechanical properties are basically similar, indicating that the modification effect of GF-L and GF-S at 20% filling amount is not much different, so subsequent test results only show the test data of GF-S.

Figures 3(a) and 3(b) show DSC plots for the heating and cooling of samples. Crystallization and melting parameters of the samples were summarized in Table 2. It can be seen from Figure 3(a) that the crystallization temperature (T_{cp}) of PP/WBG and PP/GF is higher than that of pure

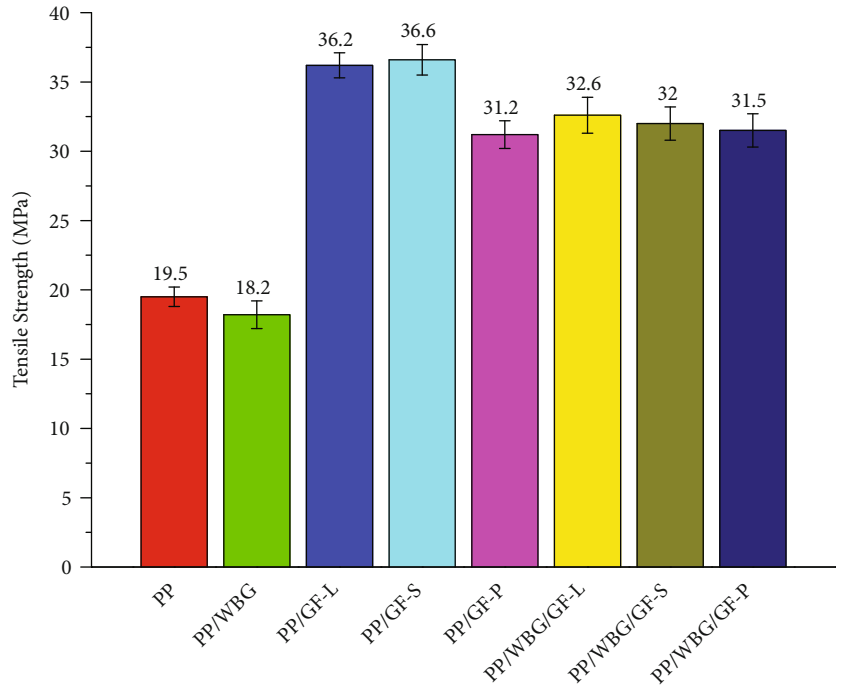

(a)

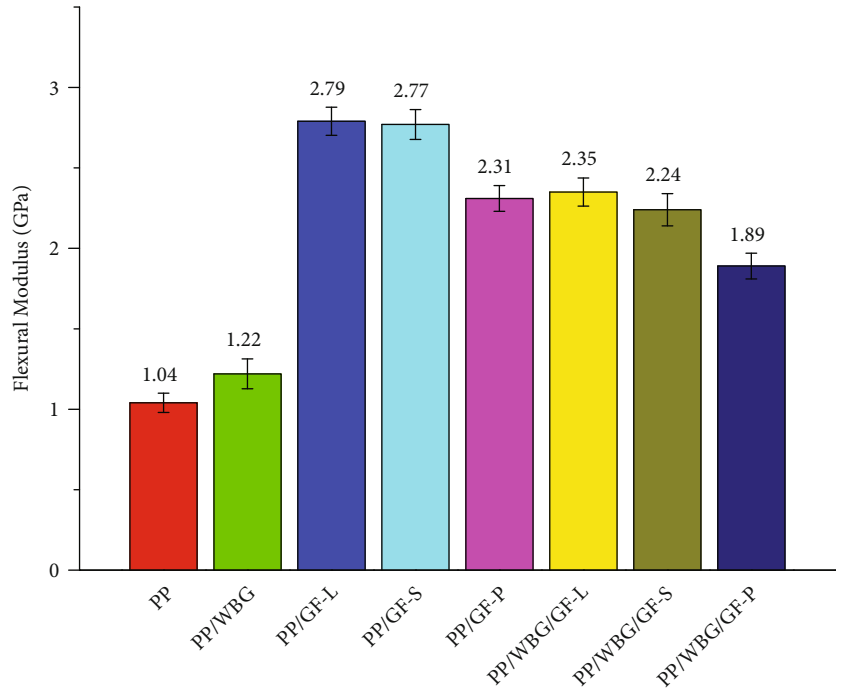

(b)

Figure 5: Continued.

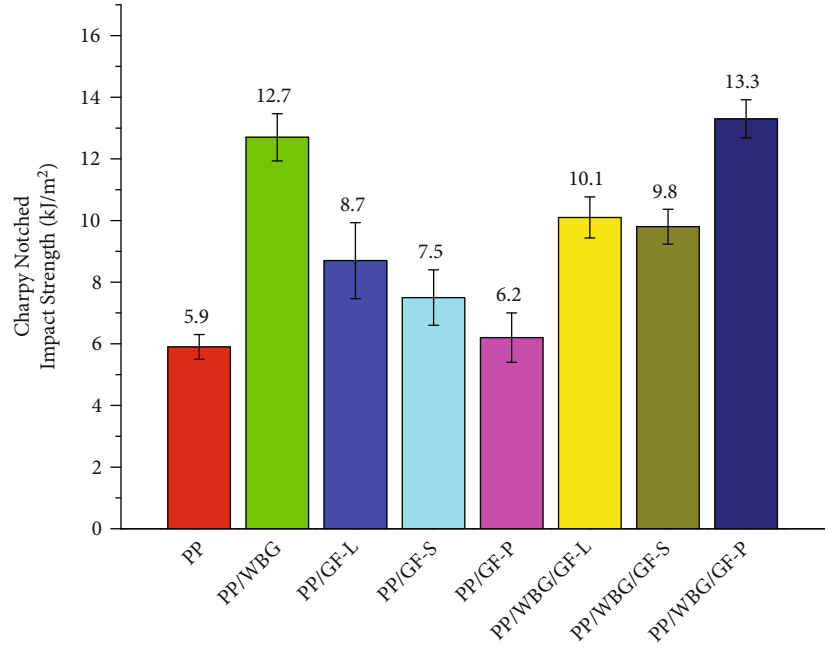

(c)

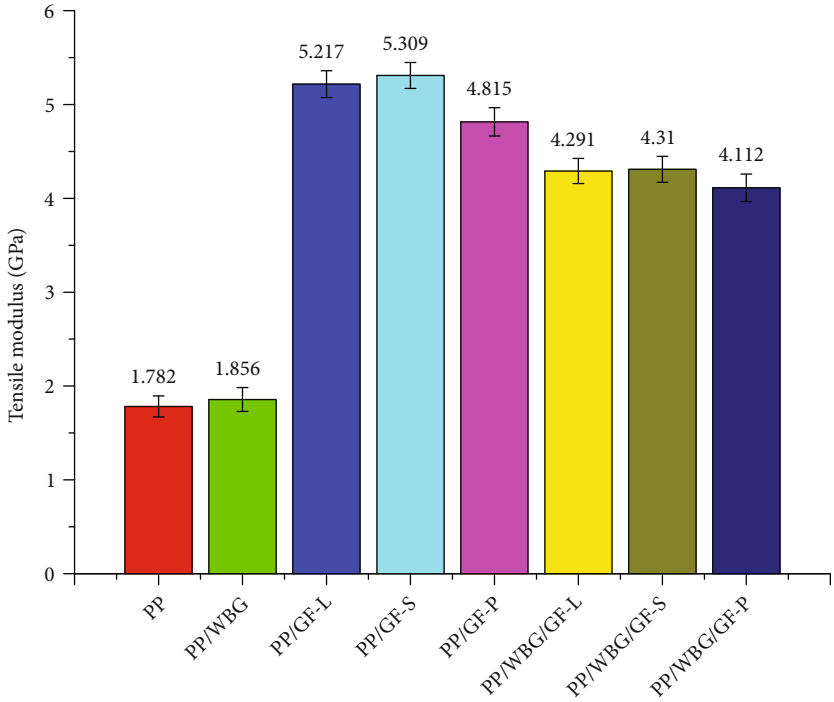

(d)

Figure 5: Continued.

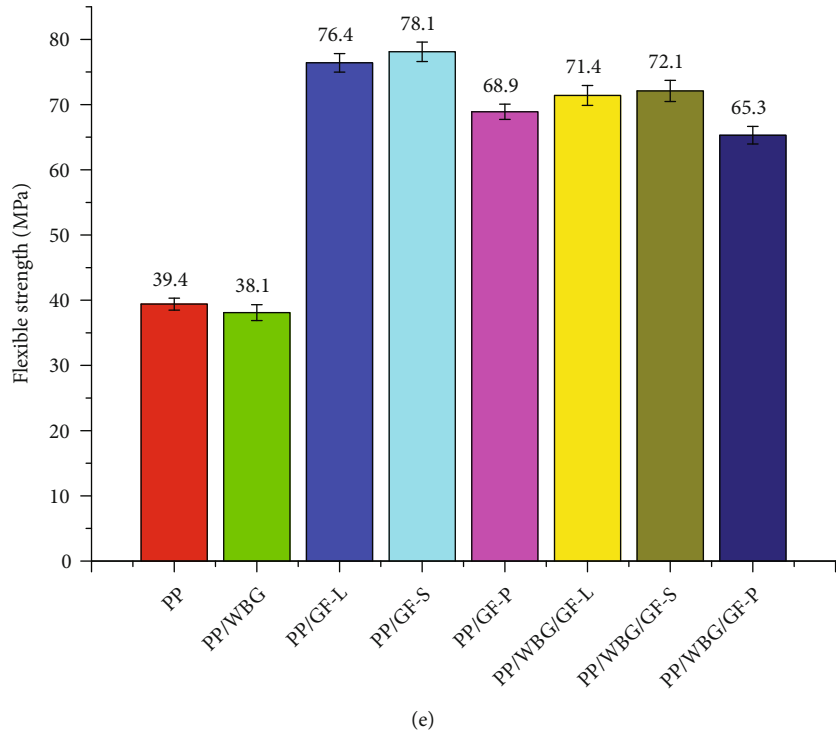

(e)

Figure 5: The tensile strength (a), flexural modulus (b), impact strength (c), tensile modulus (d), and flexible strength (e) of samples.

PP, indicating that after modified by β-NA, the crystallinity is improved, and the increase of crystallization temperature also means the improvement of well temperature resistance, which has been widely proved in previous studies [24–27]. After the addition of the nucleating agent, the T_{cp} increased from 119.2°C to 124.9°C, which was the largest relative increase, and indicated that the β crystallization in PP had a certain promoting effect on increasing the T_{cp} [28]. For PP/GF, it can be seen that T_{cp} of PP/GF-P is slightly higher than PP/GF-S, which may be due to the small amount of β crystallization produced by GF-P, and the presence of β crystallization makes the T_{cp} slightly increased, the same trend occurs in PP/WBG/GF-P and PP/WBG/GF-S. Through the results of Mai et al. [29], it was proved that the T_{cp} of Nano-$CaCO_3$ (2.0 wt%)/β-NA (0.1 wt%)/PPR increased from 105.6°C to 111.3°C compared with 2.0 wt% $CaCO_3$/PPR of unadded β-NA, indicating that the crystallization temperature can be further increased by β-NA in the presence of nanomaterials. In this study, GFP combined with nucleating agent-modified PP also obtained similar research conclusions. ΔH_c is the enthalpy of crystallization obtained by integrating from the DSC spectrum, reflecting the degree of crystallinity of different crystals in PP. It can be seen that the corresponding ΔH_c of PP/WBG added β-NA has increased, but decreased after the addition of GF, which is consistent with the changing trend of T_{cp}.

The β crystallization can be observed more clearly from the DSC heating curve in Figure 3(b). There are two distinct response peaks on the way, of which the peak corresponding to the lower temperature is the β-crystal, and the peak corresponding to the higher temperature is the α-crystal. It can be seen that PP/WBG with β-NA has a significant β-crystal response, and its $\Delta H_{\beta m}$ reaches 62.8 J/g, the largest of all samples. In the PP/GF-S sample, no β-crystal response was found, but for the PP/GF-P, a small amount of β-crystal response was found, which again indicated that the GF-P has a certain ability to promote the formation of β-crystals, which is confirmed by the results of XRD. After the addition of β-NA, PP/WBG/GF-S and PP/WBG/GF-P have an obvious β-crystal response, indicating that GFP can work synergistically with β-NA to make the β response more intense.

Many nanoparticles have the effect of promoting PP crystallization, such as zinc oxide [30], montmorillonite [31], nanocarbon [32], calcium carbonate [33], calcite [34], nanogold [35], etc., these particles play a similar role in the process of forming crystallization. Through this study, it can be seen that GFP also plays a similar role in the process of modifying PP, which can promote the formation of β crystallization.

Figure 4 shows the change of X_t over time, and some areas in the figure are enlarged for easy observation. In the X_t vs. time plot, the time required to complete half of the crystallization is defined as $t_{1/2}$, with a smaller $t_{1/2}$ representing a faster crystallization rate. The $t_{1/2}$ results of different samples are listed in Table 3, and it can be seen that the pure PP crystallization rate is relatively the slowest, while PP/WBG modified by β-NA has the highest crystallization rate. The crystallization rate of PP/GF-S and PP/GF-P has accelerated relative to PP, but the difference is less. Compared with GF filling, after the addition of β-NA, the crystallization rate increasing of PP/WBG/GF-P and PP/WBG/GF-S is relatively large, among which PP/WBG/GF-P is more obvious, which shows that GFP cooperates with β-NA can not only increase the β crystallization ratio but also have a high

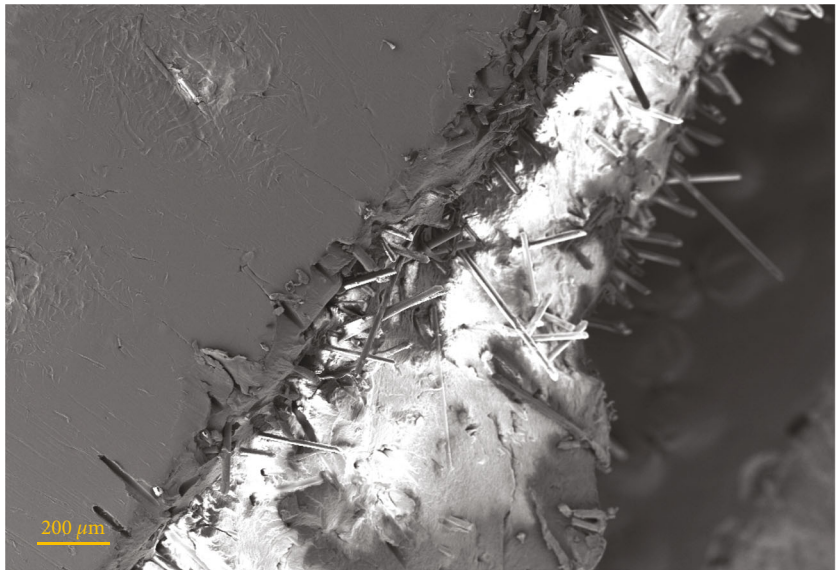

(a)

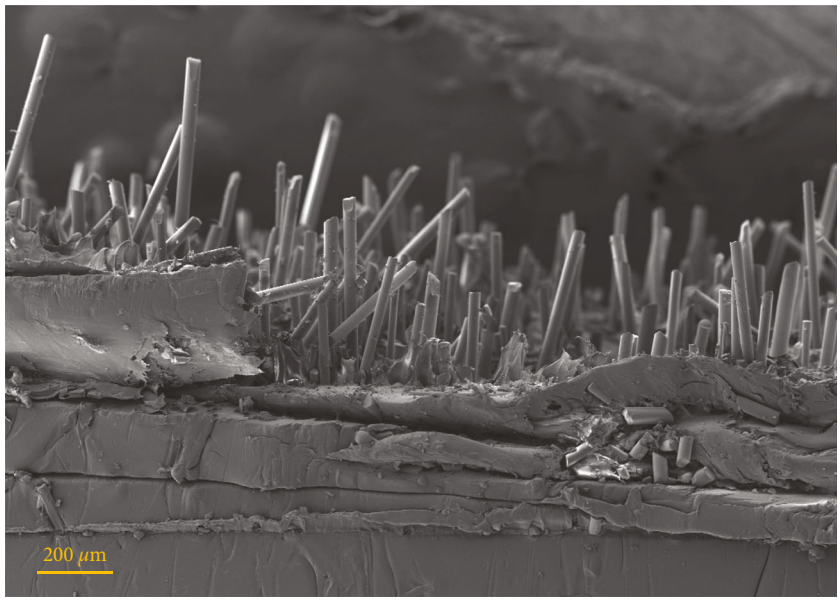

(b)

Figure 6: Continued.

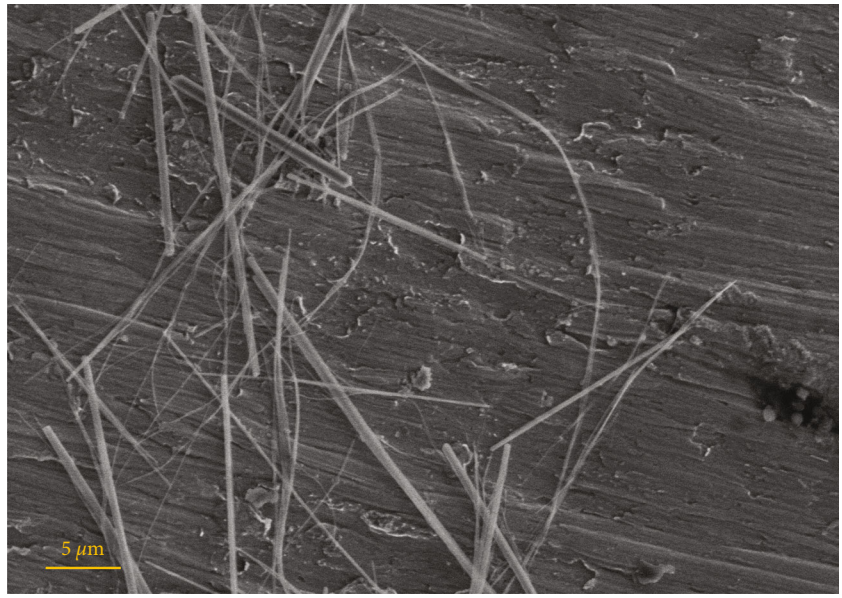

(c)

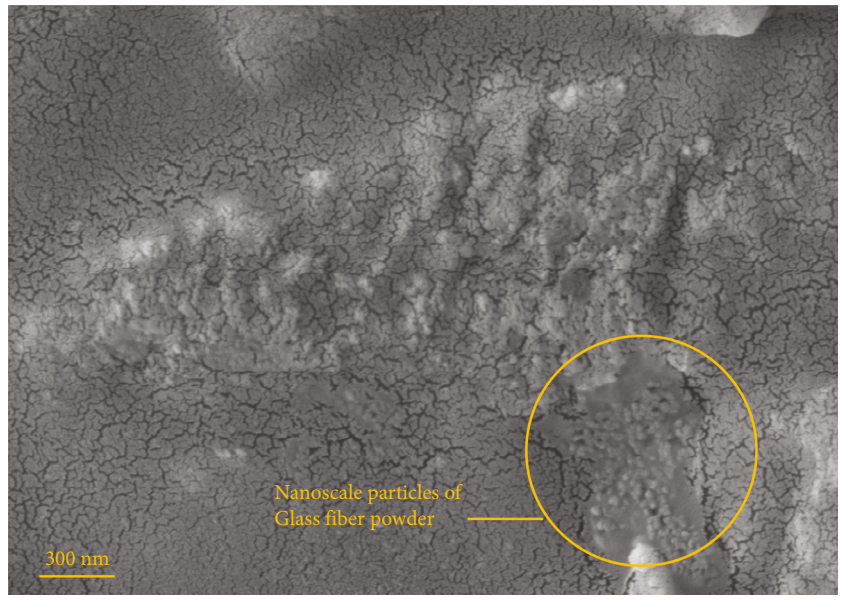

(d)

Figure 6: SEM pictures of GF-S (a), GF-L (b), and GF-P (c, d) reinforced PP.

crystallization rate. Huang et al. [36] used dibenzylidene sorbitol (DBS) as β-NA and nano-calcium carbonate to modify iPP, and found that $t_{1/2}$ decreased after the addition of nano-$CaCO_3$, and $t_{1/2}$ was further reduced after cooperating nano-$CaCO_3$ with DBS. Shentu et al. [37] found that oleic acid-modified calcium carbonate-filled PP can increase the crystallization rate of composites. All these show that whether nanomaterials are used alone or in synergy with nucleating agents, they can promote the shortening of the crystallization rate, which is also consistent with the conclusions of this study.

3.2. Mechanical Properties. PP/GF has a significant increase in rigidity properties such as tensile strength and flexural modulus. It can be seen from the previous part of this study that the crystallization properties are different in terms of crystallization characteristics for GF modification and GF synergistic β-NA-modified PP, which means that it will have different effects on the mechanical properties. The test results of tensile strength, flexural modulus, and Charpy notched impact strength of samples are shown in Figure 5. It can be seen from the results that the tensile strength and flexible strength of PP/WBG are slightly reduced compared to pure PP, tensile modulus is basically the same, but the impact strength increases significantly. Moderate amounts of β-NAs are known to have a toughening effect, but slightly reduce rigidity [38, 39]. After adding long GF and short GF to PP, the tensile strength of PP/GF-L and PP/GF-S

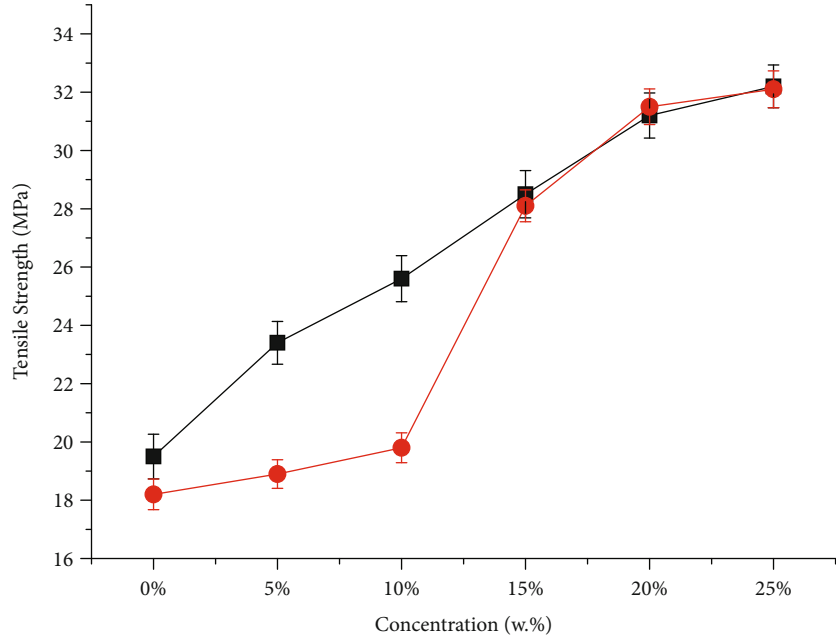

(a)

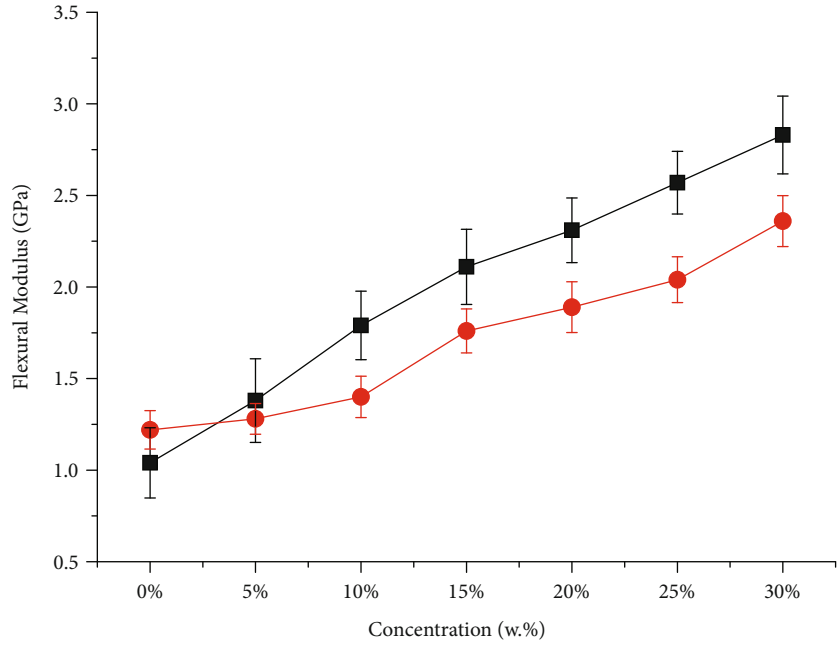

(b)

Figure 7: Continued.

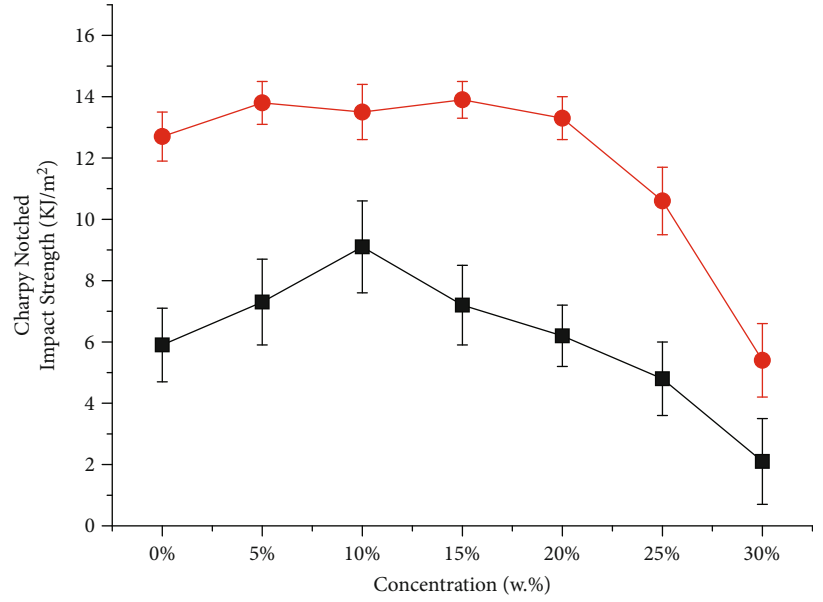

(c)

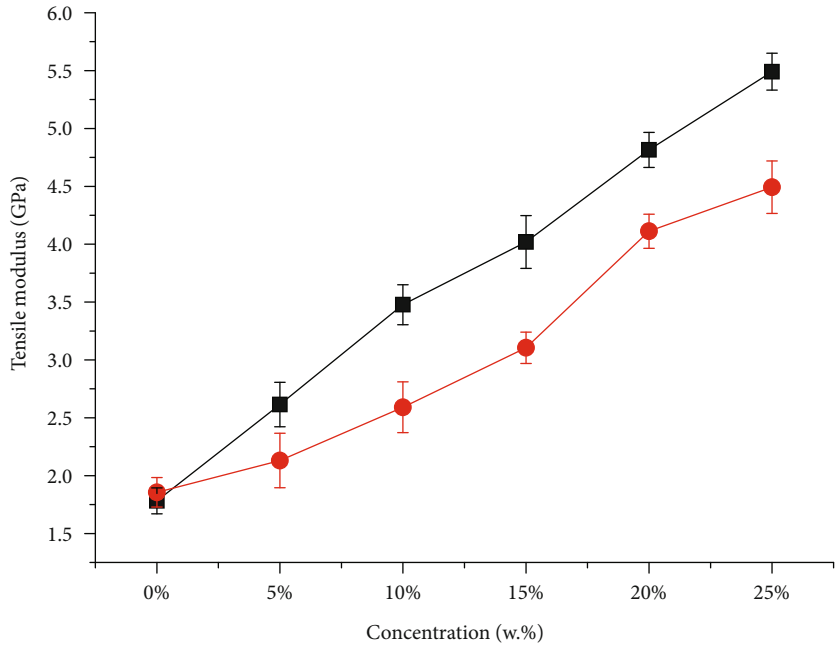

(d)

Figure 7: Continued.

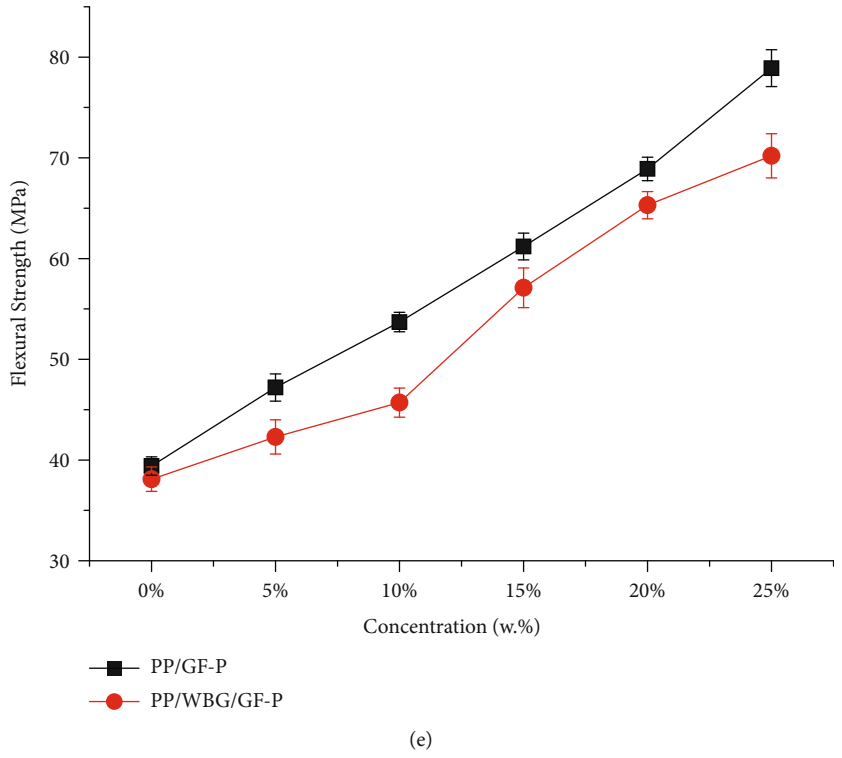

Figure 7: The tensile strength, flexural modulus, impact strength, tensile modulus, and flexible strength versus glass fiber power wt% concentration. The concentration of β-NA is fixed at 0.2%.

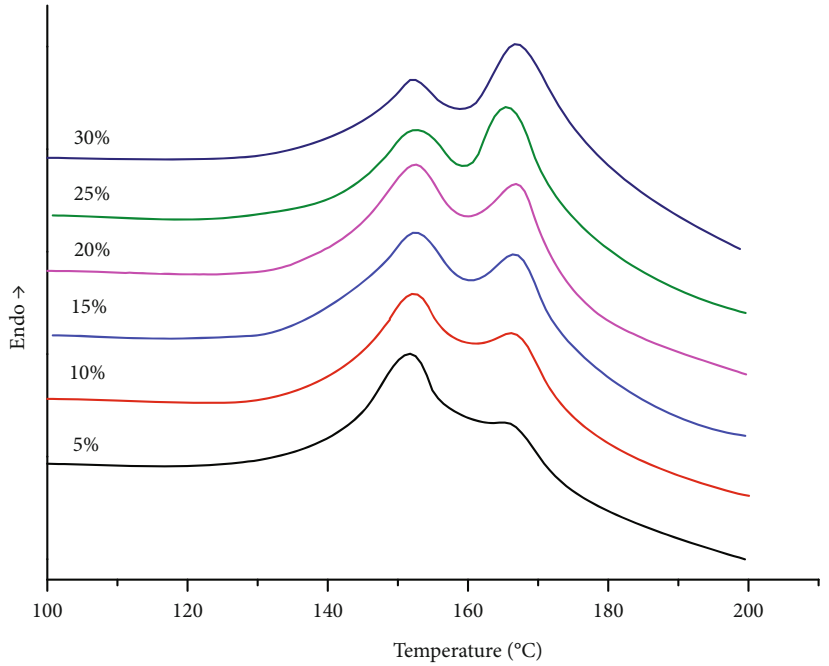

Figure 8: DSC heating curves of PP/WBG/GF-P at different GF-P wt% concentration.

increased by 1.86 times and 1.88 times, the flexural modulus increased by 2.68 times and 2.66 times, tensile modulus and flexible strength also increased significant, which means the rigidity properties increased significantly, and in terms of toughness, the notched impact strength also increased to a certain extent compared with pure PP. Compared with long and short GFs, all mechanical properties of GFP reinforced PP are reduced, which may be due to the different modification mechanisms of two-dimensional materials and one-dimensional materials on PP. It can be seen from the DSC heating curve of Figure 3(b) that the β crystallization response of PP/GF-P strength is weak, and a small amount

Table 4: Crystallization and melting parameters of PP/WBG/GF-P at different GF-P wt% concentration.

Concentration (wt%)	5	10	15	20	25	30
$T_{\beta m}$ (°C)	166.0	166.9	167.1	167.4	166.1	167.4
$\Delta H_{\beta m}$ (J/g)	143.2	119.7	115.4	109.4	82.9	74.8

of β crystallization cannot effectively enhance the toughness of the composite.

For PP modificated by GF and β-NA, tensile strength, flexural modulus, tensile modulus, and flexible strength are reduced compared to PP/GF, but can still be maintained at a relatively high level. In particular, the tensile strength of PP/WBG/GF-P is maintained at the same level as PP/WBG/GF-L and PP/WBG/GF-S, only a small reduction in other stiffness properties, and the impact strength increases significantly, reaching 13.3 kJ/m^2, which is 2.25 times that of pure PP. These can show that GFP cooperates with β-NA and has good balance stiffness–toughness performance.

The synergistic modification of PP by nanomaterials and β-NA to improve stiffness and toughening performance has been widely studied. Chen et al. [40] used carbon nanotubes (CNTs) and β-NAs to modify iPP/Styrene Ethylene Butylene Styrene (SEBS), and found that the toughness was increased by 22.3 times compared with iPP. Zhang et al. [41] found that after adding 0.05 wt% β-NA and CNT, the presence of a small amount of β crystal will break the macroscopic agglomeration of CNT and form a certain α-crystal, and this effect will have an impact on the impact strength and significantly improve the electrical conductivity and heat resistance of the composite. Zhang et al. [42] used nano-$CaCO_3$ and β-NA to modify PP, and found that the presence of β-NA would make nano-$CaCO_3$ disperse better, and the interaction between β-crystal and nano-$CaCO_3$ would form α-crystals, which would affect the performance of the composites. In this study, both mechanical properties and crystallization properties also show that the GFP and β-NA have a synergistic modification effect.

3.3. SEM Observation. Figures 6(a) and 6(b) show the Scanning Electron Microscope (SEM) pictures of GF-S and GF-L reinforced PP, from which that can be seen cut GF can be clearly observed at the cross-section of both PP materials, which is caused by the strong shear force when GF extruded in the twin-screw extruder. Compared to the good isotropy of GFs in GF-L, the GFs in GF-S reinforced PP are more heterogeneous and non-isotropic. Figure 6(c) shows the surface of the GF-P reinforced PP material, and it can be seen that GFs of several tens of microns in length are embedded in the PP surface. When magnifying the observation to the nanometer level, it can be seen from the surface of the GF-P reinforced PP material in Figure 6(d) that there are agglomerated nanometer-sized particles filled in, which are finer particles of GFP.

3.4. GFP Concentration. To further study the synergistic modification effect between GF-P and β-NA, in this study, the GF-P concentration was changed with or without β-NA, and the effects on mechanical properties were investigated, results were shown in Figure 7. It can be seen that all of the stiffness properties (tensile strength, flexural modulus, tensile modulus, and flexible strength) of the sample without β-NA increase linearly with the GF concentration. After the addition of β-NA, when the GF concentration is below 10 wt%, the tensile strength increases more slowly, but when the GF concentration reaches 15 wt%, the tensile strength increases significantly, and keeps with the level of PP/GF in the further higher GF concentration. The flexural strength, tensile modulus, and flexible strength of PP/WBG/GF-P increase linearly with the GF concentration, but it is lower than that of PP/GF-P in the investigated scope. In terms of notched impact strength, PP/GF-P without β-NA increased firstly and then decreased with the increase of GF concentration, reaching a maximum at 10 wt% GF concentration. After adding the β-NA, when the GF-P concentration is less than 20 wt%, the impact strength has been maintained at a high stable level, which indicates that the synergistic effect of GFP and β-NA can maintain a high level of toughness when the content of GFP is relatively high.

Figure 8 shows the DSC heating curves of samples with different GF concentrations in PP/WBG/GF-P, and the relevant $\Delta H_{\beta m}$ and $T_{\beta m}$ are summarized in Table 4. It can be seen that with the increase of GF concentration, the β-crystal response intensity and $\Delta H_{\beta m}$ gradually decrease, but within 20 wt% GF concentration, it remains at a high level. When the GF-P concentration reaches 25 wt% or 30 wt%, the β-crystal response intensity and $\Delta H_{\beta m}$ decrease amplitude is accelerated. The decrease in β-crystal response intensity means the decreasing of impact strength, which confirms the trend of impact strength under different GF-P concentrations in Figure 7(c). Wang et al. [22] found that the content of nano-SiO_2 in iPP reached about 4%, and the impact strength and flexural strength will reach to the maximum. According to GFP particle size distribution from Figure 1, it can be deduced that a small amount of nano-scale SiO_2 may play the role of nucleating agent, and other micron-level SiO_2 plays a filling and stiffening effect, when the amount of nano-scale SiO_2 of in GF-P exceeds the optimal content, it will cause a decrease in β crystallization content, which may be the reason for the reduction of the toughness in PP with high-content GFP.

4. Conclusion

PP/GF is widely used in various fields. In this article, the influence of GF materials with different shapes and lengths on the properties of modified PP was investigated, and found that GF-P can play the role of β-NA compared with other GF, the existence of β-crystals in PP can effectively improve the toughness properties. As a rule, the ways of producing β-crystals in PP include nucleating agent modification and nanoparticle filling, when the β-NA is used alone, the toughness will increase by the decreasing of rigidity. For the nanoparticle filling modification, the cost always is high, and the problems of agglomeration and uneven mixing

are easy to occur during preparation [43–45]. Therefore, GF-P reinforced PP can achieve the comprehensive performance of rigidity and toughness, with a lower cost, and the continuous process of preparation is easy to achieve, which is of great application significance for the improvement of toughness for traditional PP.

The conclusions are summarized as follows:

(1) The particle size distribution of GFP is wide, in which the finer particles can play a certain role of nucleating agent.

(2) Combine β-NA with GF to reinforce PP, which can further improve the crystallization transformation of β, especially for GFP has good balance stiffness–toughness performance.

(3) The optimal GF concentration has a relative scope, which is within ≤20 wt% in this study, and excessive content will reduce the β crystallization content and notched impact strength.

(4) The average length of GF has little effect on the mechanical properties and characters of modified PP.

Data Availability

The data used to support the findings of this study are currently under embargo while the research findings are commercialized. Requests for data, 12 months after publication of this article, will be considered by the corresponding author.

Conflicts of Interest

The authors declare that they have no conflicts of interest.

Acknowledgments

The authors are grateful for the support of the Science and Technology Department of Ningxia Hui Autonomous Region, China (Grant: 2020BDE2017).

References

[1] J. L. Thomason and M. A. Vlug, "Influence of fibre length and concentration on the properties of glass fibre-reinforced polypropylene: 1. Tensile and flexural modulus," *Composites Part A: Applied Science and Manufacturing*, vol. 27, no. 6, pp. 477–484, 1996.

[2] J. L. Thomason, "The influence of fibre length and concentration on the properties of glass fibre reinforced polypropylene: 7. Interface strength and fibre strain in injection moulded long fibre PP at high fibre content," *Composites Part A: Applied Science and Manufacturing*, vol. 38, no. 1, pp. 210–216, 2007.

[3] J. L. Thomason, "The influence of fibre length and concentration on the properties of glass fibre reinforced polypropylene. 6. The properties of injection moulded long fibre PP at high fibre content," *Composites Part A: Applied Science and Manufacturing*, vol. 36, no. 7, pp. 995–1003, 2005.

[4] J. L. Thomason and W. M. Groenewoud, "The influence of fibre length and concentration on the properties of glass fibre reinforced polypropylene: 2. Thermal properties," *Composites Part A: Applied Science and Manufacturing*, vol. 27, no. 7, pp. 555–565, 1996.

[5] J. L. Thomason and M. A. Vlug, "Influence of fibre length and concentration on the properties of glass fibre-reinforced polypropylene: 4. Impact properties," *Composites Part A: Applied Science and Manufacturing*, vol. 28, no. 3, pp. 277–288, 1997.

[6] J. L. Thomason, "The influence of fibre length and concentration on the properties of glass fibre reinforced polypropylene: 5. Injection moulded long and short fibre PP," *Composites Part A: Applied Science and Manufacturing*, vol. 33, no. 12, pp. 1641–1652, 2002.

[7] J. L. Thomason, M. A. Vlug, G. Schipper et al., "Influence of fibre length and concentration on the properties of glass fibre-reinforced polypropylene: Part 3. Strength and strain at failure," *Composites Part A: Applied Science and Manufacturing*, vol. 27, no. 11, pp. 1075–1084, 1996.

[8] G. Luo, W. Li, W. Liang et al., "Coupling effects of glass fiber treatment and matrix modification on the interfacial microstructures and the enhanced mechanical properties of glass fiber/polypropylene composites," *Composites Part B: Engineering*, vol. 111, pp. 190–199, 2017.

[9] R. Watanabe, A. Sugahara, H. Hagihara et al., "Insight into interfacial compatibilization of glass-fiber-reinforced polypropylene (PP) using maleic-anhydride modified PP employing infrared spectroscopic imaging," *Composites Science and Technology*, vol. 199, p. 108379, 2020.

[10] Y. Jin, C. Xin, Y. He et al., "The effect of nano-silica modified glass fiber on the properties of glass fiber reinforced polypropylene composites," *Journal of Beijing University of Chemical Technology*, vol. 47, no. 2, p. 36, 2020.

[11] A. Zheng, H. Wang, X. Zhu et al., "Studies on the interface of glass fiber-reinforced polypropylene composite," *Composite Interfaces*, vol. 9, no. 4, pp. 319–333, 2002.

[12] X. Y. Dai and P. J. Bates, "Mechanical properties of vibration welded short-and long-glass-fiber-reinforced polypropylene," *Composites Part A: Applied Science and Manufacturing*, vol. 39, no. 7, pp. 1159–1166, 2008.

[13] M. Z. Rong, M. Q. Zhang, Y. X. Zheng et al., "Improvement of tensile properties of nano-SiO_2/PP composites in relation to percolation mechanism," *Polymer*, vol. 42, no. 7, pp. 3301–3304, 2001.

[14] W. Wu, M. H. Wagner, and Z. Xu, "Surface treatment mechanism of nano-SiO_2 and the properties of PP/nano-SiO_2 composite materials," *Colloid and Polymer Science*, vol. 281, no. 6, pp. 550–555, 2003.

[15] L. Huang, R. Zhan, and Y. Lu, "Mechanical properties and crystallization behavior of polypropylene/nano-SiO_2 composites," *Journal of Reinforced Plastics and Composites*, vol. 25, no. 9, pp. 1001–1012, 2006.

[16] G. Sodeifian, S. Ghaseminejad, and A. A. Yousefi, "Mechanical and morphological properties of polypropylene/short glass fiber/POE-g-MA composite manufactured by fused deposition modeling (FDM) and CM methods," *The 10th International Chemical Engineering Congress & Exhibition (IChEC 2018)*, pp. 1–5, 2018, Isfahan, Iran, 6-10 May.

[17] A. K. Gupta, K. R. Srinivasan, and P. K. Kumar, "Glass fiber reinforced polypropylene/EPDM blends. II. Mechanical properties and morphology," *Journal of Applied Polymer Science*, vol. 43, no. 3, pp. 451–462, 1991.

[18] S. E. Barbosa, N. J. Capiati, and J. E. M. Kenny, "Processability and mechanical properties of ternary composites PP/EPDM/GF," *Polymer Composites*, vol. 21, no. 3, pp. 377–386, 2000.

[19] D. Mi, R. La, T. Wang et al., "Hierarchic structure and mechanical property of glass fiber reinforced isotactic polypropylene composites molded by multiflow vibration injection molding," *Polymer Composites*, vol. 38, no. 12, pp. 2707–2717, 2017.

[20] L. Cui, P. Wang, Y. Zhang et al., "Glass fiber reinforced and β-nucleating agents regulated polypropylene: a complementary approach and a case study," *Journal of Applied Polymer Science*, vol. 135, no. 5, p. 45768, 2018.

[21] Z. He, Y. Zhang, and Y. Li, "Dependence of β-crystal formation of isotactic polypropylene on crystallization condition," *Journal of Polymer Research*, vol. 27, no. 9, pp. 1–9, 2020.

[22] D. Wang, Y. Feng, L. Han et al., "Effect of wet surface treated nano-SiO_2 on mechanical properties of polypropylene composite," *Journal Wuhan University of Technology, Materials Science Edition*, vol. 23, no. 3, pp. 354–357, 2008.

[23] J. X. Li and W. L. Cheung, "On the deformation mechanisms of β-polypropylene: 1. Effect of necking on β -phase PP crystals," *Polymer*, vol. 39, no. 26, pp. 6935–6940, 1998.

[24] W. H. Ruan, Y. L. Mai, X. H. Wang et al., "Effects of processing conditions on properties of nano-SiO_2/polypropylene composites fabricated by pre-drawing technique," *Composites Science and Technology*, vol. 67, no. 13, pp. 2747–2756, 2007.

[25] A. Hassan, N. A. Rahman, and R. Yahya, "Extrusion and injection-molding of glass fiber/MAPP/polypropylene: effect of coupling agent on DSC, DMA, and mechanical properties," *Journal of Reinforced Plastics and Composites*, vol. 30, no. 14, pp. 1223–1232, 2011.

[26] S. Li, S. Sun, H. Liang et al., "Production and characterization of polypropylene composites filled with glass fibre recycled from pyrolysed waste printed circuit boards," *Environmental Technology*, vol. 35, no. 21, pp. 2743–2751, 2014.

[27] H. M. Miao, Y. B. Xu, F. X. Zhang et al., "A comparative study on recycled glass fibers and milled glass fibers as reinforcement fibers in polypropylene," *Advanced Materials Research*, vol. 955–959, pp. 2625–2628, 2014, https://doi.org/10.4028/www.scientific.net/AMR.955-959.2625.

[28] Q. Dou, "Effect of the composition ratio of pimelic acid/calcium stearate bicomponent nucleator and crystallization temperature on the production of β crystal form in isotactic polypropylene," *Journal of Applied Polymer Science*, vol. 107, no. 2, pp. 958–965, 2008.

[29] J. H. Mai, M. Q. Zhang, M. Z. Rong et al., "Crystallization behavior and mechanical properties of nano-$CaCO_3$/β-nucleated ethylene-propylene random copolymer composites," *Express Polymer Letters*, vol. 16, pp. 739–749, 2012.

[30] J. Tang, Y. Wang, H. Liu et al., "Effects of organic nucleating agents and zinc oxide nanoparticles on isotactic polypropylene crystallization," *Polymer*, vol. 45, no. 7, pp. 2081–2091, 2004.

[31] A. Pozsgay, T. Frater, L. Papp et al., "Nucleating effect of montmorillonite nanoparticles in polypropylene," *Journal of Macromolecular Science, Part B*, vol. 41, no. 4–6, pp. 1249–1265, 2002.

[32] S. Reyes-de Vaaben, A. Aguilar, F. Avalos et al., "Carbon nanoparticles as effective nucleating agents for polypropylene," *Journal of Thermal Analysis and Calorimetry*, vol. 93, no. 3, pp. 947–952, 2008.

[33] Y. Lin, H. Chen, C. Chan et al., "Nucleating effect of calcium stearate coated CaCO3 nanoparticles on polypropylene," *Journal of Colloid and Interface Science*, vol. 354, no. 2, pp. 570–576, 2011.

[34] M. Gahleitner, C. Grein, and K. Bernreitner, "Synergistic mechanical effects of calcite micro-and nanoparticles and β-nucleation in polypropylene copolymers," *European Polymer Journal*, vol. 48, no. 1, pp. 49–59, 2012.

[35] R. Masirek, E. Szkudlarek, E. Piorkowska et al., "Nucleation of isotactic polypropylene crystallization by gold nanoparticles," *Journal of Polymer Science Part B: Polymer Physics*, vol. 48, no. 4, pp. 469–478, 2010.

[36] Y. Huang, G. Chen, Z. Yao et al., "Non-isothermal crystallization behavior of polypropylene with nucleating agents and nano-calcium carbonate," *European Polymer Journal*, vol. 41, no. 11, pp. 2753–2760, 2005.

[37] B. Shentu, L. Jipeng, and W. Zhixue, "Effect of oleic acid-modified nano-CaCO3 on the crystallization behavior and mechanical properties of polypropylene," *Chinese Journal of Chemical Engineering*, vol. 14, no. 6, pp. 814–818, 2006.

[38] H. Bai, Y. Wang, Z. Zhang et al., "Influence of annealing on microstructure and mechanical properties of isotactic polypropylene with β-phase nucleating agent," *Macromolecules*, vol. 42, no. 17, pp. 6647–6655, 2009.

[39] S. Zhao and Z. Xin, "Nucleation characteristics of the $\alpha\beta$ compounded nucleating agents and their influences on crystallization behavior and mechanical properties of isotactic polypropylene," *Journal of Polymer Science Part B: Polymer Physics*, vol. 48, no. 6, pp. 653–665, 2010.

[40] Y. Chen, Z. Wu, Q. Fan et al., "Great toughness reinforcement of isotactic polypropylene/elastomer blends with quasi-cocontinuous phase morphology by traces of β-nucleating agents and carbon nanotubes," *Composites Science and Technology*, vol. 167, pp. 277–284, 2018.

[41] Y. Zhang, H. Liu, L. Zhang et al., "Improved conductivity and thermal stability by the formation of a charge-transfer complex in β-nucleation-agent-nucleated and MWCNT-filled iPP composites," *Journal of Applied Polymer Science*, vol. 129, no. 5, pp. 2744–2753, 2013.

[42] Y. Zhang, H. Liu, L. Zhang et al., "Influence of β nucleation agent on the dispersion of nano-$CaCO_3$ in isotactic polypropylene matrix," *Journal of Applied Polymer Science*, vol. 128, no. 5, pp. 3382–3389, 2013.

[43] D. Bikiaris, "Microstructure and properties of polypropylene/carbon nanotube nanocomposites," *Materials*, vol. 3, pp. 2884–2946, 2010.

[44] M. A. Bhuiyan, R. V. Pucha, J. Worthy et al., "Understanding the effect of CNT characteristics on the tensile modulus of CNT reinforced polypropylene using finite element analysis," *Computational Materials Science*, vol. 79, pp. 368–376, 2013.

[45] M. A. Bhuiyan, R. V. Pucha, J. Worthy et al., "Defining the lower and upper limit of the effective modulus of CNT/polypropylene composites through integration of modeling and experiments," *Composite Structures*, vol. 95, pp. 80–87, 2013.